Permafrost-Glacier Interaction – Process Understanding of Permafrost Reformation and Degradation

Jan-Christoph Otto [(1)] **& Markus Keuschnig** [(1,2)]

[(1)] *Department of Geography and Geology, University of Salzburg, Salzburg, Austria*
[(2)] *alpS – Centre for Climate Change Adaptation, Innsbruck, Austria*

1 Introduction

The dramatic changes of mountain glaciers and significant rock fall events during exceptional warm summers in the last decades have strongly raised awareness and interest in changing geomorphologic conditions of high mountain areas. Alpine areas are considered to be particularly sensitive to climate change and observations as well as projections report a rise of temperatures significantly above lowland areas (Bogataj 2007). Temperature increase in high mountain areas affects glacier and permafrost distribution and causes reactions on geomorphological as well as hydrological conditions. Most permafrost areas in high mountains are located in close vicinity to glaciers due to similar environmental requirements. The strong loss of length and volume of Alpine glaciers represent the most visible manifestation of cryosphere change in high mountains. While glacier changes become apparent in relatively short reaction times, mountain permafrost reacts also sensitive to warming but somewhat delayed and almost invisible. The major objective of this study is to investigate the condition and evolution of the ground thermal regimes in glacial and periglacial environments after glacier melt.

The scientific communities of glacier and permafrost research have operated separately in the past, even though, interactions between glaciers and permafrost are recognised (Haeberli 2005). Many equilibrium lines of Alpine glaciers in continental climates are located within zones of permafrost occurrence (Haeberli & Gruber 2008). Thus, the thermal regimes of surface ice and frozen ground can be interconnected influencing each other. Glaciers may exhibit cold or polythermal conditions at the base mainly as a function of energy and mass balance at the surface or influence of negative temperatures from below due to the existence of permafrost (Suter et al. 2001). In the Swiss Alps cold based glacier occurrence is assumed to be restricted to altitudes above 3,800 m (Haeberli 1976; Suter 2001). The occurrence of hanging glaciers and ice patches on steep bedrock slopes of the highest peaks is associated with cold based conditions and the occurrence of permafrost (Haeberli 2005). Disappearing hanging glaciers and ice covered steep slopes during the last century may be the result of warming subsurface conditions within the steep rock walls. However, little is known on this relationship due to scarce data on bedrock permafrost or ice wall thermal conditions (Ravanel & Deline 2011).

Glacier retreat has released significant areas since the last glacier maximum during the Little Ice Age (mid-19th century). With the continuing melt of Alpine glaciers significant space is released at altitudes potentially susceptible for permafrost existence. This space is either located in front of the glacier (forefield) due to length reduction of the glacier or surrounding the glacier due to reduction of glacier thickness. In these areas various polygenetic ground ice occurrences have been observed. The origin of the ice has been assigned to three processes: (Type I) refreezing of former unfrozen glacier beds (i. e. formation of permafrost), (Type II) preservation of previous subglacial permafrost and (Type III) burial of dead ice (Kaab & Kneisel 2006; Kneisel 2003; Kneisel & Kaab 2007; Lugon et al. 2004). However, little is known on the time required for formation of permafrost in Alpine environments (Lunardini 1995) or the preservation of permafrost below glacier coverage. The interpretation of differing observations concerning permafrost thawing and degradation and potential natural hazards (e. g. rock falls, debris flows) remains a major challenge (Haeberli et al. 2010). Efficient risk analysis and risk adaptation strategies depend largely on process understanding of permafrost-related evolution and related hazards. Permafrost degradation is one potential effect of warming trends in the Alps (APCC 2014) leading to destabilisation of bedrock slopes and increased potential of debris slow generation (Sattler et al. 2011). However, in order to assess the future impact of permafrost areas to the formation of natural hazards due to climate change, knowledge of the glacier-permafrost interaction is required. This includes understanding of the different reaction times of glaciers and permafrost zones to temperature increase. If glacier melt happens faster than subsurface warming we could experience an incre-

Figure 1: View of the Schmiedingerkees glacier below Kitzsteinhorn peak (center left)

ase in permafrost area in high Alpine terrain previously covered by glacier ice. This would also increase the hazard potential in these areas and needs to be considered for planning of adaptation strategies (Keuschnig et al. 2011).

This study aims at understanding the permafrost-glacier relationship in the Kitzsteinhorn area, Kaprun, Austria (Fig. 1). By analysing both the recent history of glacier ice change and the current occurrence of permafrost and its thermal state and conditional parameters (climate, land surface parameters) we aim to understand the existence or permafrost conditions in the direct vicinity of the glacier. The main research questions include:

- What are the ground thermal conditions around the Schmiedingerkees glacier?
- Can we observe and identify permafrost occurrence?
- When did the permafrost locations become exposed from the glacier cover?
- Which factors influence the ground thermal conditions around the Schmiedingerkees glacier?

2 Test site

The study is located at the Schmiedingerkees cirque at the Kitzsteinhorn ski area in the Federal Province of Salzburg, Hohe Tauern Range, Austria. The cirque opens in north-eastern direction from the summit of the Kitzsteinhorn (3,203 m), covering approximately 3 km² and a vertical elevation difference of 1,500 m between the summit and the glacier forefield limits (1,700 m maximum Little Ice Age extent). The Kitzsteinhorn is located just north of the main Alpine divide and has no directly adjacent summits. The Schmiedingerkees glacier has a size of approximately 1.05 km² (2012), covering around 40% of the cirque area. The glacier is a flat cirque type glacier surrounded by steep bedrock slopes of up to 250 m height (Fig. 3).

The Kitzsteinhorn area primarily consists of calcareous mica schists (Höck & Pestal 1994). Stress release and intense physical weathering processes, typical for periglacial environments, resulted in the formation of an abundance of joint sets with large apertures in the rock walls of the peak and adjacent cirque walls. Intense retreat of the Schmiedingerkees glacier in recent decades led to the exposure of oversteepened rock faces, which in turn are frequently affected by minor rock fall events (Hartmeyer et al. 2012). The recently exposed glacier forefield is characterised by large areas of exposed bedrock (Fig. 3). Only lateral and lower parts are debris covered and

Table 1: Climate data of the reference climate stations around the Kitzsteinhorn

Location	Altitude [m]	Time period	MAAT [°C]	Mean snow height [m]	Max snow height [m]	Mean solar radiation [W / m²]
Alpincenter	2,446	01.2005–08.2013	0.78	0.93	2.8	–
Kammerscharte	2,561	11.2008–08.2013	–3.23	1.2	3.6	166.8
Glacier Plateau	2,910	11.2008–08.2013	–2.99	1.5	4.1	–

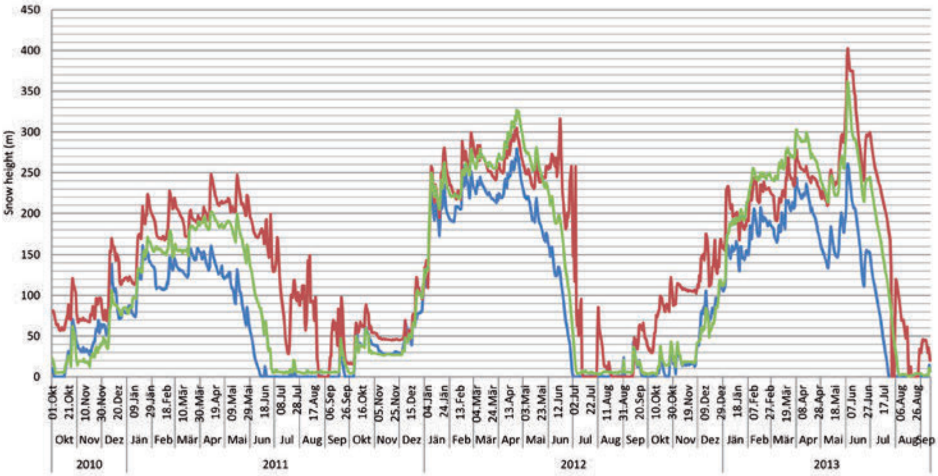

Figure 2: Snow height measurement at the three climate stations in the study area between 2010 and 2013

contain surface indicators for previous glacier extent (lateral, frontal moraines). Apparently, the Schmiedingerkees has a low debris production compared to other glaciers. The largest area of thick debris cover is located in the eastern part of the glacier forefield, east of the Schmiedinger lake. The steep cirque side walls are characterised by intense rock fall and avalanche activity. Especially the eastern ridge, descending from the Kitzsteinhorn peak shows intense erosion leading to debris cover of the eastern part of the glacier. This debris input is most probably responsible for the debris accumulation in the forefield at the eastern side. Prominent lateral moraines that indicate the Little Ice Age (LIA) maximum can be observed south of the Alpincenter (2,446 m) and within the descending valley north of the lake. Three weather stations are located within the study area, permitting continuous observation of external forcing of ground thermal conditions. The weather stations are located at the Alpincenter (2,446 m) of the ski station at the Kammerscharte (2,561 m) in the neighbouring cirque towards the southeast and directly on the Schmiedingerkees glacier (2,940 m). The stations show mean annual air temperature (MAAT) values of 0.8 °C, –3.2 °C and –3.0 °C, respectively. The large variability could be the result of local influences on the measurement, for example the impact of warming from the building at the Alpincenter may result in an increase in MAAT. Maximum snow heights between 2.8 and 4.1 m are recorded between 2005 and 2013 (Table 1, Fig. 2).

The tourism infrastructure existing within the study area (cable car, ski lifts, ski slopes, etc.) provides easy access and convenient transportation of measuring equipment, an essential prerequisite for an extensive long-term monitoring program (Keuschnig et al. 2011). However, the glacier forefield is strongly affected by the intense usage and modification of the terrain for the construction of ski slopes, roads and buildings thus having an impact on debris characteristics and ground thermal condition. Since most of the skiing is performed on the glacier itself, the station ma-

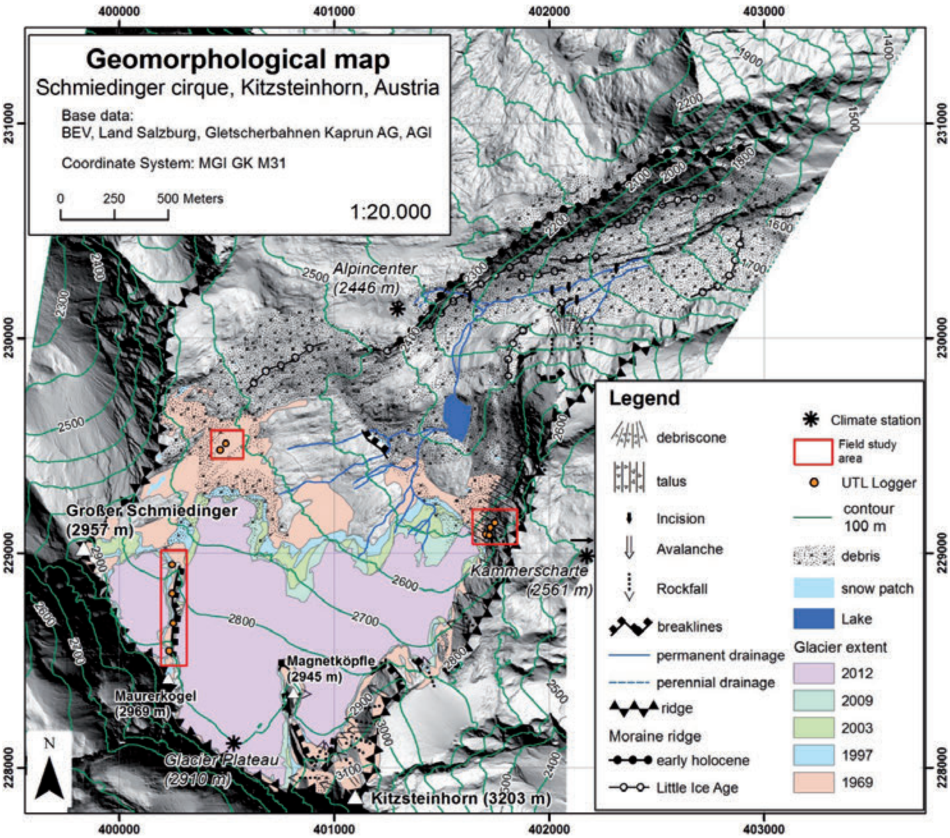

Figure 3: Geomorphological map of the Schmiedingerkees cirque, Kitzsteinhorn, Kaprun, Austria

nagement also involves the glacier conditions by constructions of ski slopes, filling of crevasses and lifts tracks on the ice. In order to minimise direct human impact on the subsurface conditions we chose two locations close to the glacier where little or no construction works or surface modification was performed.

3 Methods

The study combines field data with remote sensing and Geographical Information System (GIS) analysis and is split into research on the changes of the glacier forefield induced by glacier retreat and investigation on the permafrost occurrence and the measurement of surface / subsurface temperatures.

The field work comprises permafrost detection by electrical resistivity tomography (ERT) and measurement of surface / subsurface temperatures using data loggers.

Resistivity measurements were performed using a GeoTomMK8E1000[1] multi-electrode resistivity system with 24 electrodes and 2 to 4 m electrode spacing. ERT was analysed with the Res2DInv software package.

For the collection of ground surface temperature (GST) data we placed ten Universal Temperature Loggers (UTL) (Type UTL1, Geotest.ch, ex-factory accuracy of ± 0.1 °C) in the top layer (–5 to –10 cm) of the subsurface. Temperature loggers were placed at three different locations at various altitudes and on different subsurface conditions (fine grain material, coarse grain material, and close to bedrock) and where covered by fine grain sediments to avoid direct exposure to the sun and snow. Additionally, we could use climate data from three climate stations in the Kitzsteinhorn area, recording temperature, precipitation, snow height, solar radiation and wind. All climate and temperature data was stored and analysed using a Microsoft Access database. We derived mean annual ground surface temperature (MAGST), winter equilibrium temperature (WEqT), duration of snow cover (SCD) and estimated time since deglaciation for all GST locations. MAGST is calculated for entire years if available and the entire data set. In case of missing records we added the missing days from neighbouring locations with similar data as previously applied by Apaloo et al. (2012). WEqT is generally considered as stable temperature during the longest continuous duration of thick snow cover (> 50 cm) over a minimum duration of two weeks (Schoeneich 2011). Snow height measurements at the surrounding climate stations indicate a thick snow cover of at least 1 m or more for most of the winter until at least May at wind sheltered locations (Fig. 2). The formation of a WEqT and the interpretation of WEqT conforming to the Bottom Temperature of the Snow cover (BTS) principle should therefore be possible for our logger sites (Schoeneich 2011). WEqT were extracted by visual inspection of the temperature data timelines in the database. Morphometric land surface characteristics have been calculated (slope, aspect, and total insolation) for the logger sites to analyse external location influences. SCD quantification is based on observations made by Schmidt et al. (2009) who identified a standard deviation of less than 0.3 K of GST during 24 h as good indicator of snow coverage. Additionally, we estimated the time since deglaciation based glacier extent visible on the aerial imagery available.

For the GIS and remote sensing analyses different digital elevation models (DEM) and different aerial images have been collected. Geomorphological features have been mapped using airborne laser scanning (ALS) data (Land Salzburg and Gletscherbahnen Kaprun AG) with 1 m resolution and high resolution aerial imagery (2012, Land Salzburg). Data on glacier extends have been generated by mapping on digital orthophotos from 1982, 1997, 2003, 2009 and 2012 (Land Salzburg). Glacier extent from 1969 was extracted from the Austrian Glacier Inventory (Gross 1987). Morphometric landform parameters have been calculated in ArcGIS and SAGA GIS using 1 m ALS DEM and a 5 m x 5 m analysis window to eliminate local derivation.

[1] http://geolog2000.de (17.12.2013)

Figure 4: Historical images (postcards) showing the glacier extend of the Schmiedingerkess below the Kitzsteinhorn. The postcard on the right is marked with 15. August 1906 (Verlag Würthle & Sohn, Salzburg, No. 208), the image on the left is dated to 1933 (Bergwelt Verlag, C. Jurischek, Salzburg; historical images kindly provided by Heinz Slupetzky, Salzburg). The glacier terminus has reached the cirque boundary. The glacier is filling large parts of the cirque and has a connection to the Kammerkees glacier towards the eastern flank of the Kitzsteinhorn peak. Also visible is a pronounced ice cover on the steep slopes of the peak. The Magnetköpfle, a small peak towards the right of the Kitzsiteinhorn seems to be almost completely ice covered in 1906. In contrast the Maurergrat ridge, visible on the right image in the upper right part of the Schmiedingerkees glacier was only partially covered with ice.

4 Results

4.1 Changes of the Schmiedingerkees glacier area

The Schmiedingerkees has experienced a total loss of around 70% of area covered at the LIA maximum (Table 2). The length change is about 2.4 km since the LIA and 300 m since the onset of length records in 1951 (WGMS 2012). During its LIA maximum the glacier is terminated in a pronounced tongue at an altitude of approximately 1,635 m above Kaprun valley, leaving the cirque area. Based on morphological mapping, the maximum extent of the glacier could be reconstructed. For area calculation it is assumed that the glacier ice filled the cirque to a great portion leaving only higher parts of the surrounding cirque walls free of ice. Since early 20th century the glacier was restricted to the cirque area and changed into a flat cirque glacier with no pronounced glacier tongue (Fig. 4). The glaciers lost an average of 15,000 m^2 of area per year between LIA and 2012. In the last years (2009–2012), this number has doubled.

The melting of the glacier released an area of 2.4 km^2 since the LIA at altitudes between 1,635 and 3,200 m. Strongest changes in glacier area are by nature observed in the lower part of the glacier, but significant area is released of ice in the upper parts as well (Fig. 5). Especially the existence of glacier ice on the steep northern rock wall of the Kitzsteinhorn that existed until the 1980s has released significant surface here.

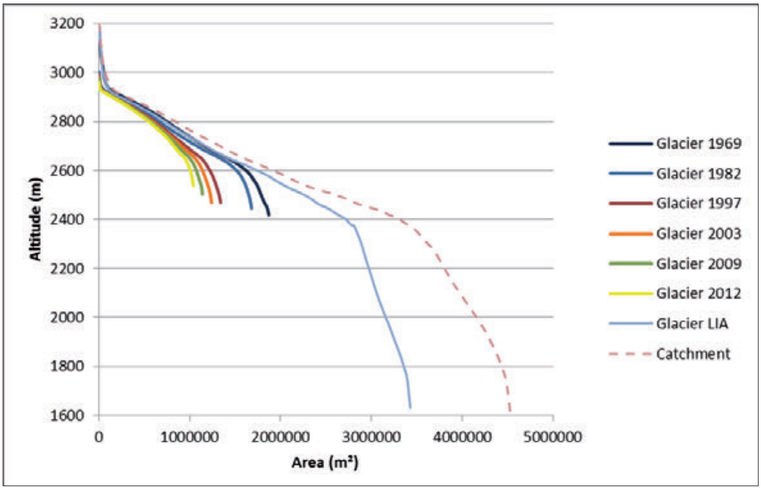

Figure 5: Hypsometric curve of the Schmiedinger glacier area between LIA and 2012. Data based on 1 m DEM (Land Salzburg and Gletscherbahnen Kaprun AG), geomorphological mapping and digital orthophoto analysis

4.2 Permafrost evidences

4.2.1 Ground surface temperature data

The GST loggers have been placed in the eastern and western part of the glacier forefield as well as on the Maurergrat, a ridge separating the Schmiedingerkees from the Maurerkees in the west (Fig. 3). In the glacier forefield east, loggers are located on a steep talus deposit of fine to coarse grain size (unfortunately these logger only recorded data from one hydrological year due to technical failure). The loggers are placed at altitudes between 2,534 m and 2,546 m within a distance of 30 m. The location is assumed to be free of glacier ice a maximum of 40 years (Table 3). But it is like-

Table 2: Glacier area changes of the Schmiedingerkees based on geomorphological mapping and orthophoto interpretation

Year	Area [km²]	Change to previous date [km²]	%	Change to LIA maximum [km²]	%
LIA (assumed 1850)	3.4	0	0	0	0
1969	1.88	−1.5	44.7	−1.5	−44.7
1982	1.69	−0.2	9.9	−1.7	−50.2
1997	1.34	−0.4	20.7	−2.1	−60.5
2003	1.24	−0.1	7.6	−2.2	−63.5
2009	1.15	−0.1	7.6	−2.3	−66.3
2012	1.05	−0.1	8.6	−2.4	−69.2

ly that this slope previously contained remains of the debris covered glacier tongue until a few years ago. Impressive stripes of the debris, visible on the aerial images, correspond to the previous movement of the glacier ice. In the western part of the glacier forefield loggers are placed on little inclined terrain in small pockets of fine sediments between polished bedrock outcrops at altitudes of 2,631 m and 2,623 m. This terrain is assumed to be free of ice since 15 to 30 years based on the aerial images. The GST loggers located on the Maurergrat ridge also placed in small pockets

Table 3: Land surface parameters of the GST data loggers

Location	Recording period	Altitude [m]	Slope [°]	Aspect [°]	Surface cover	Ruggedness Index	Total Insolation per year [kWh / m²]	Estimated time since deglaciation
Glacier forefield East								
UTL-2087	09.11–07.12	2,538	39.8	303.5	Talus slope, fine grain sediment, close to bedrock	0.59	1,278.1	Max.40
UTL-707	09.11–02.13	2,534	37.1	289.5	Talus slope, fine grain sediment	0.53	1,442.3	Max.40
UTL-759	09.11–12.12	2,546	38.4	297.0	Talus slope, fine grain sediment, close to bedrock	0.56	1,354.9	Max.40
UTL-702	09.11–07.12	2,537	37.2	306.7	Talus slope, fine grain sediment	0.54	1,293.0	Max. 40
Glacier forefield West								
UTL-2104	09.09–10.12	2,631	18.6	124.1	glacier forefield, medium grain sediment, close to bedrock	0.24	2,227.1	15–30
UTL-2092	09.09–10.12	2,623	17.1	15.5	glacier forefield, medium grain sediment, close to bedrock	0.23	1,531.6	15–30
Maurergrat								
UTL- 2067	09.09– 9.12	2,915	14.5	336.0	Ridge, fine grain sediment, close to bedrock	0.18	1,794.4	Max.44
UTL- 2091	09.09–10.12	2,878	2.1	261.8	Ridge, fine grain sediment, close to bedrock	0.14	2,139.9	Max. 44
UTL-2095	09.09–05.12	2,847	19.1	302.3	Ridge, fine grain sediment, close to bedrock	0.25	1,811.5	Max. 44
UTL-2074	09.09–09.12	2,775	49.5	316.5	Ridge, fine grain sediment, close to bedrock	0.84	958.1	Max. 44

Table 4: Ground thermal data of the logger sites

Location	Altitude [m]	MAGST [°C]	Time period for MAGST	WEqT [°C] [year]	Mean duration of snow cover [days]
Glacier forefield east					
UTL-2087	2,538	1.02	09.2011–09.2012	−1.3 [2011]	224
UTL-707	2,534	0.00	09.2011–09.2012	−2.3 [2011]	225
UTL-759	2,546	1.04	09.2011–09.2012	−2.3 [2011]	245
UTL-702	2,537	1.40	09.2011–09.2012	−1.2 [2011]	255
Glacier forefield west					
UTL-2104	2,631	2.12	09.2009–09.2012	−1.2 [2012]	245
UTL-2092	2,623	0.72	09.2009–09.2012	−1.9 [2012]	279
Maurergrat ridge					
UTL- 2067	2,915	−0.52	09.2009–09.2011	−3.8 [2012]	302
UTL- 2091	2,878	−1.17	09.2009–09.2011	−4.1 [2012]	315
UTL-2095	2,847	−1.71	09.2009–09.2011	−3.4 [2010]	124.5
UTL-2074	2,775	−1.58	09.2009–09.2011	−4.5 [2010]	222

of fine sediment in close proximity to the bedrock outcrop. These loggers are placed along an altitudinal transect just of the western side of the ridge at altitudes between 2,775 m and 2,915 m. The loggers are approximately 130 m apart from each other. The western part of the ridge has been covered by glacier ice observable on the aerial photos of 1969. Apparently the ridge was never completely ice covered (see Fig. 4 right). It is assumed that the bedrock of the east facing rock wall was free of ice during LIA maximum extent.

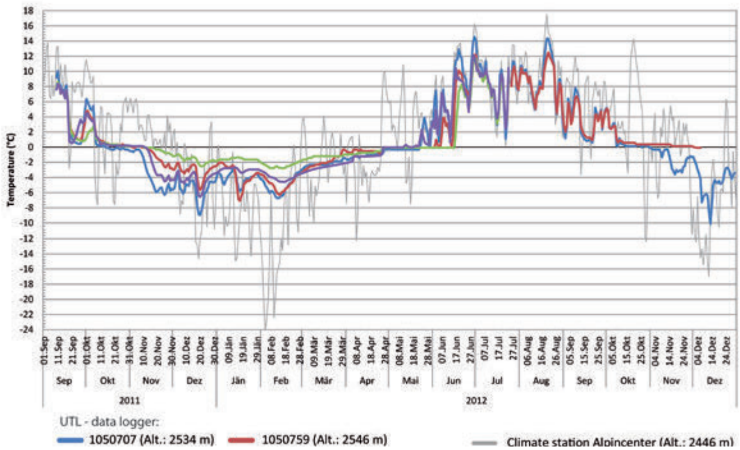

Figure 6: GST recorded between Sept. 2011 and Dec. 2013 at Glacier Forefield East and air temperature measured at the Alpincenter climate station

The MAGST for all logger locations is presented in Table 4. The loggers placed along the Maurergrat ridge have MAGST values below zero indicating potential permafrost conditions, at all other locations MAGST is at or above zero degrees. A closer look at the annual variation in GST is presented in Figures 6 to 8. At the Glacier Forefield East (GFE) all loggers show a typical early winter temperature variation following roughly daily temperature changes (Fig. 6). Snow cover starts to develop in early October and lasts until end of May observable by the zero curtain

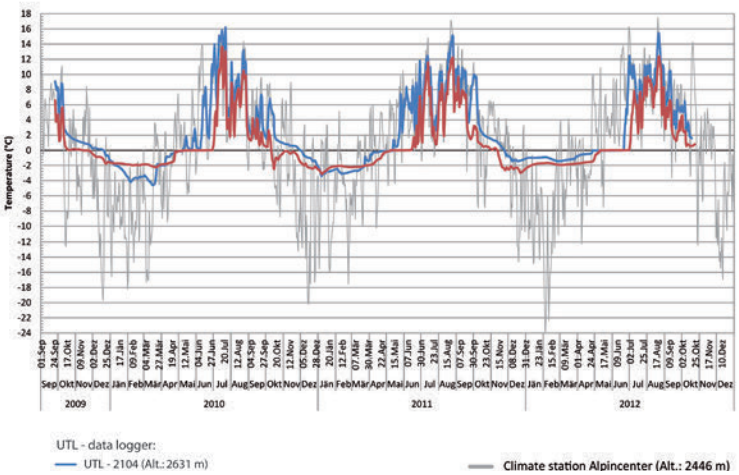

Figure 7: GST recorded between Sept. 2009 and Oct. 2012 at Glacier Forefield West and temperature data measured at the Alpincenter climate station

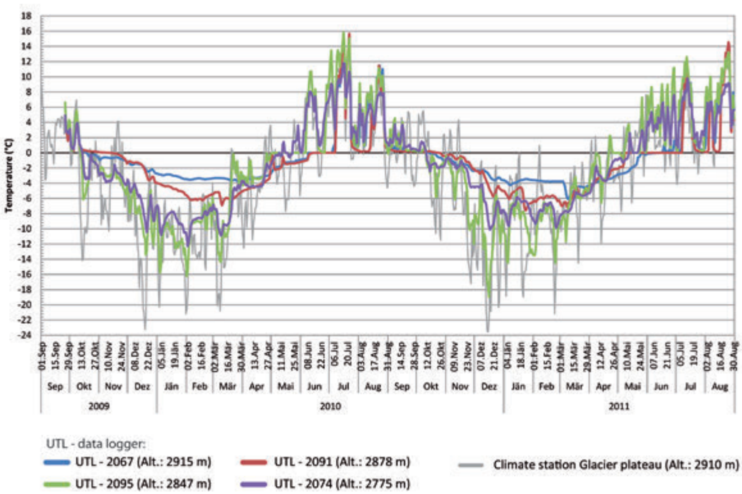

Figure 8: GST recorded between Sept. 2009 and Aug. 2011 at Maurergrat ridge and temperature data measured at the glacier plateau climate station

effect in the data, corresponding to snow height measurements at the neighbouring climate stations. However, only two loggers have smooth winter curves (UTL 2087, UTL 1050702) indicating a better isolation effect of the snow cover here that allows for a development of a WEqT. We extracted a WEqT at these locations between –1.2 °C and –2.3 °C indicating that this is a boundary location where permafrost is possible.

At the Glacier Forefield West (GFW) we have three years of winter recording (2009 to 2011) and smoother winter curves compared to the situation at glacier forefield east (Fig. 7). Both loggers reveal very stable temperature conditions indicating a thick permanent snow cover and little impact from air temperature. Onset of snow cover lies between the 8th and 17th of October between 2009 and 2011. It is observable that the general trends between the lines change from year to year with generally colder temperatures at UTL 2104 (blue curve) in winter 2010 and parts of winter 2011 and a higher temperatures in 2012. This could be related to the effect of snow cover at the two sites. At site UTL 2091 (red curve) the late winter zero curtain is much longer compared to the neighbouring site and lasts till mid-June. This indicates a thicker snow cover that may also be responsible for quite stable GST values between January and April. This location seems to be better sheltered protecting the snow cover from wind and sun more than the other location nearby. The long period of zero curtain effect could also be responsible for the significant lower MAGST compared to site UTL 2104. Though MAGST is positive, WEqT of –1.9 °C indicates that this location has a weak potential to provide permafrost conditions.

At the Maurergrat ridge GST is recorded since 2009 and the last data was gathered in 2011. Here, two locations (UTL 2067 and UTL 2091) show smooth winter curves compared to the other two locations that show strong variations during winter (Fig. 8). The latter locations (UTL 2095 and UTL 2074) seem to have less thick snow cover recognisable in missing of a pronounced zero curtain effect at the end of the winter. Since the loggers are located close to the ridge it is very likely that wind erosion of snow play a major role here. All loggers show MAGST temperatures between –0.5 and –1.7 °C giving a clear indication for permafrost conditions. Since measurement conditions at UTL 2095 and UTL 2074 seem to be strongly affected by wind activity leading to a removal of the isolating snow cover, determination of WEqT is difficult at these sites. We therefore only discuss WEqT at the sites UTL 2067 and UTL 2091. At these two locations WEqT of –3.8 and –4.0 °C, respectively, are clear indicators of permafrost condition.

4.2.2 Resistivity data

Resistivity measurements have been performed at various locations in the glacier forefield and on the Maurergrat ridge (Fig. 3). Figure 9 depicts the resistivity conditions at GFE within a few meters to the actual glacier terminus. The profile runs from the debris covered glacier tongue (left) towards north-east into the proglacial debris (right). The resistivity values are between 1,000 and >1,000,000 Ωm. The resistivity distribution clearly marks the transition between the glacier ice with values above 100,000 Ωm and the non-frozen zone in the proglacial area with values

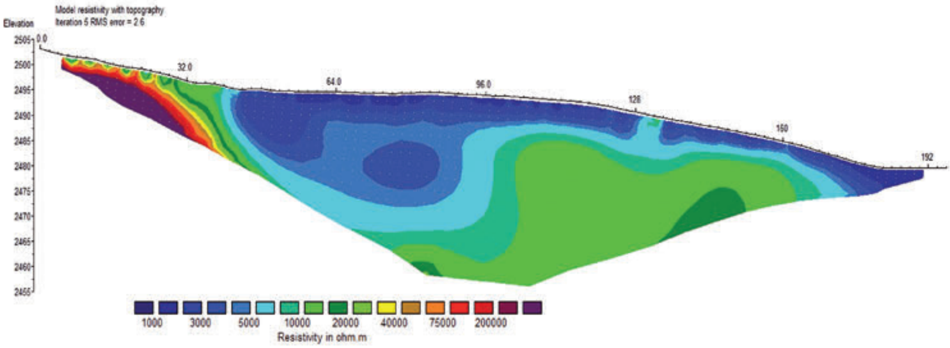

Figure 9: Resistivity measurement at GFE

< 20,000 Ωm. Two other measurements at this part of the glacier forefield produced a similar image. Based on resistivity measurements it is unlikely that permafrost conditions are present in the eastern part of the deglaciated area at an altitude of 2,490 to 2,530 m on a northeast exposed slope.

In contrast, clear permafrost evidence by high resistivity values can be observed on the ridge of the Maurerkogel at altitudes between 2,875 and 2,950 m (Fig. 10). The measurement reveals a clear horizontal layering of resistivity values with a distinct rise above 20,000 Ωm in about 5 to 8 m depth. Resistivity data here depicts a typical Alpine late summer permafrost situation (date of measurement Sept. 2009) with an unfrozen active layer (resistivity < 20,000 Ωm) and permafrost conditions indicated by resistivity values of >10,000 Ωm. This ERT profile runs parallel to the location of the GST loggers at the ridge and backs up the GST observation.

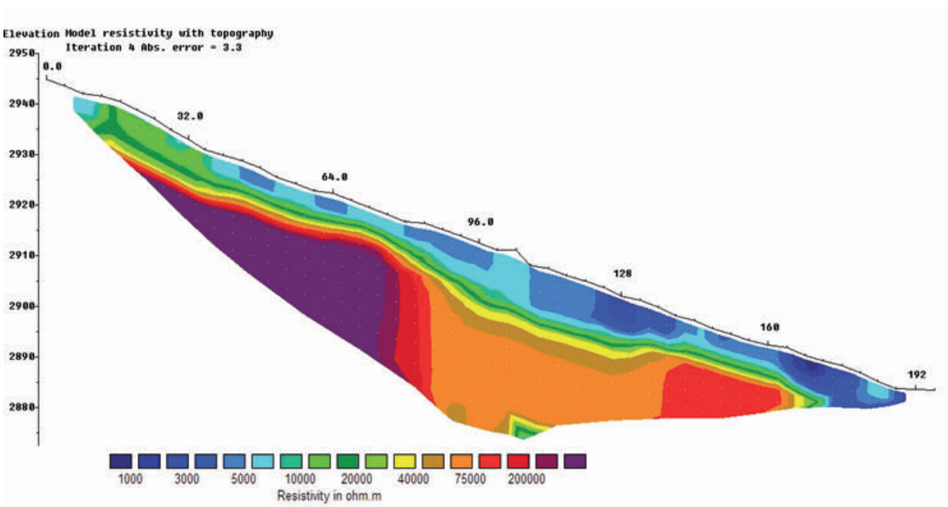

Figure 10: Resistivity measurement on the Maurergrat ridge

4.2.3 Permafrost modelling

A statistical model of permafrost distribution (Permakart 3.0) has been applied for the Kitzsteinhorn area based on a preceding study conducted by the authors at the University of Salzburg (Permalp.at project). The model is based on empirical permafrost data from the Hohe Tauern range (Schrott et al. 2012) and presents an index of probability of permafrost occurrence. An area of 1.2 km² within the cirque of the Schmiedingerkees is potentially covered by permafrost. The model shows that large parts of the current glacier forefield lies within the potential zone for permafrost (Fig. 11). The lowest potential permafrost zones are located on steep, northern exposed slopes or isolated patches. Below 2,600 m front of the Schmiedingerkees glacier and below 2,700 m in front of the Maurerkees glacier, the probability of permafrost occurrence drops below 20%. Below 2,500 m only very isolated patches provide permafrost conditions. Both test sites in the forefield lie outside the modelled permafrost area, but are very close to lower limit modelled.

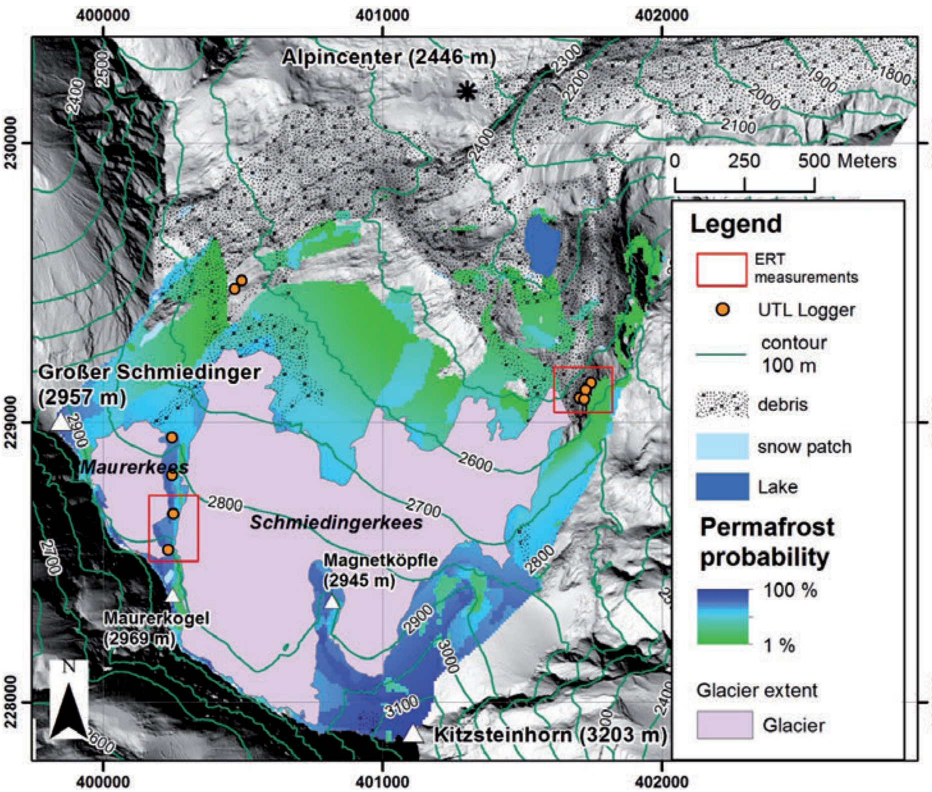

Figure 11: Map of potential permafrost distribution at the Kitzsteinhorn around the glacier extent of 2012

4.3 Discussion

Based on the permafrost model and the mapped glacier area we can identify which parts of the areas exposed by glacier melt are potentially under permafrost conditions. Assuming the same distribution of permafrost 40 years ago the potential area of permafrost condition increased from 0.5 to 1.1 km² between 1969 and 2012 by the melting of glacier ice. Looking at the altitudinal distribution of permafrost area we notice a very homogenous increase of permafrost area across the entire spread of the cirque (Fig. 12). This is related to the overall decreasing glacier thickness and the release of rock walls alongside the margins of the glacier. Additionally, the former ice cover of the Kitzsteinhorn north face produces a slightly stronger increase at the highest altitudes above 2,950 m.

While indication on permafrost presence is strong at the Maurergrat ridge we found less likely evidence for permafrost in the glacier forefield. At the Maurergrat ridge both ERT and GST data show permafrost occurrence, which is also modelled by the permafrost distribution model (Fig. 11). The ERT profile shows a pronounced permafrost body with an unfrozen top layer between 5 and 8 m depth. WEqT <–3 indicates that this top layer is refreezing during winter representing an active permafrost occurrence. ERT values show a permafrost thickness of at least 20 m below the active layer (Fig. 10). We assume that this ridge was most probably ice covered on the top during the LIA, but the eastern rock wall was still exposed and mostly ice free. We interpret this permafrost occurrence to be a preserved, pre-existing ground ice. Under these assumptions the glacier ice of the Schmiedingerkees must have been cold based when it covered parts of the Maurergrat ridge. The ground thermal conditions at this site are most likely influenced by three dimensional effects from the adjacent rock wall where negative temperature impact penetrated into the bedrock

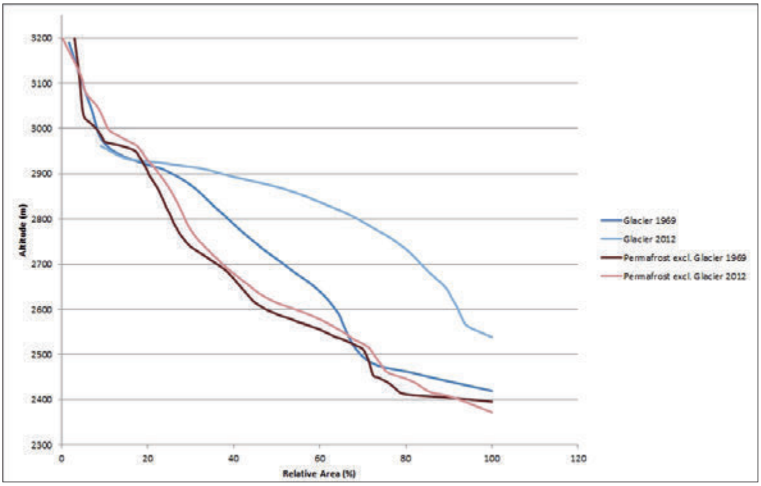

Figure 12: Hypsometry distribution of glacier ice and potential permafrost area between 1969 and 2012

ridge. Currently, the strong disturbances of the snow cover due to the exposed location and strong wind contributes to negative energy balances during most of the winter preserving the permafrost condition within the ridge.

At GFE we did not find permafrost indication in the ERT measurements. However, we assumed that until a few decades ago this slope was covered by preserved debris covered ice, similar to the current conditions only 30 m upwards. This ground ice seems to be completely vanished today. GST values however indicate a weak potential for permafrost conditions at the upper part of the slope in transition to the bedrock. This is revealed also by the permafrost model. Very low annual total radiation values below 1,400 kWh / yr. may be favouring permafrost development here. It is possible that the time period of around 40 years for permafrost formation has been too short at this location or that MAAT at this altitude is too high for formation of permafrost.

Looking at the data from GFW we can conclude that permafrost conditions are possible based on ground thermal conditions, but not verified by additional measurements. This location is less steep and receives a stronger insolation input compared to the eastern glacier forefield (Table 3). Thus, a formation of new permafrost conditions is less likely here compared to the eastern glacier forefield.

5 Conclusions

A comparison of glacier area change and permafrost distribution modeling shows that significant space has been exposed with permafrost conditions between 2,400 and 3,200 m. Additionally, we could observe a significant negative ground thermal regime indicating permafrost conditions at a ridge location between 2,770 and 2,910 m that has been partially ice covered in the past. Due to the thickness of the permafrost layer we classify this permafrost occurrence as preserved ground ice that has been in place for a long time. Current local environmental conditions contribute to the preservation of this ground ice today. In the glacier forefield WEqT data indicate a possibility for permafrost, but additional data form ERT does not reveal permafrost existence. We thus cannot identify new formation of permafrost at the glacier forefield, which is either due to too little time for formation or due to too strong positive energy input at these altitudes. A continuing of GST measurements at this boundary location is required before information on permafrost formation and the required time period is available. We therefore propose an ongoing monitoring to gain further insight into this sensitive land surface condition.

6 Outlook

In order to better understand the preservation and possible formation of permafrost conditions in glacier forefield longer time series of ground thermal data are required.

This enables to evaluate the consequences of ground thermal regime changes after surface exposure by ice melt and helps to understand the time frame at which new permafrost is build up. Based on the observations at the Schmiedingerkees glacier area we have to conclude that a large part of these potential sensitive zones are located in very steep terrain with limited accessibility. Ongoing monitoring should therefore benefit from existing logistical support from cable cars and existing infrastructure for data collection despite more human impact and disturbance at these sites.

7 Acknowledgements

This study is funded by the Austrian Academy of Science (ÖAW). This support is gratefully acknowledged. Furthermore, this investigation benefits from the close cooperation with the alpS project MOREXPERT, the logistic and financial support by the Gletscherbahnen Kaprun AG and the highly valuable help by colleagues and students in the field. We thank all supporters for their help.

8 References

Apaloo, J., A. Brenning & X. Bodin 2012: Interactions between Seasonal Snow Cover, Ground Surface Temperature and Topography (Andes of Santiago, Chile, 33.5° S). *Permafrost and Periglacial Processes* 23, 4: 277–291.

APCC (in prep.): *Österreichischer Sachstandsbericht Klimaänderungen 2014 (AAR14)*. Climate Change Centre Austria.

Bogataj, L.K. 2007: How will the Alps respond to climate change? Szenarios for the future of Alpine water. In: Psenner, R. & R. Lackner (eds.): *The Water Balance of the Alps – What do we need to protect the water resources of the Alps? Proceedings of the Conference held at Innsbruck University, 28–29 September 2006*. Innsbruck: 43–51.

Haeberli, W. 1976: Eistemperaturen in den Alpen. *Zeitschrift für Gletscherkunde und Glazialgeologie* 11, 2: 203–220.

Haeberli, W. 2005. Investigating glacier – permafrost relationships in high-mountain areas: historical background, selected examples and research needs. In: Harris, C. & J.B. Murton (eds.): *Cryospheric Systems – Glaciers and Permafrost*. Geological Society Special Publication 242. London: 29–37.

Haeberli, W. & S. Gruber 2008: Research challenges for permafrost in steep and cold terrain: an alpine perspective. In: Kane, D.L. & K.M. Hinkel (eds.): *Proceedings of the Ninth International Conference on Permafrost*, Fairbanks, Alaska, 29 June–3 July 2008. Vol. 1: 597–605.

Haeberli, W., J. Noetzli, L. Arenson, R. Delaloye, I. Gärtner-Roer, S. Gruber, K. Isaksen, C. Kneisel, M. Krautblatter & M. Phillips 2010: Mountain permafrost: development and challenges of a young research field. *Journal of Glaciology* 56, 200: 1043–1058.

Hartmeyer, I., M. Keuschnig & L. Schrott 2012: Long-term monitoring of permafrost-affected rock faces – A scale-oriented approach for the investigation of ground thermal conditions in alpine terrain, Kitzsteinhorn, Austria. *Austrian Journal of Earth Science* 105, 2: 128–139.

Höck, V. & G. Pestal 1994: *Geological map of Austria 1 : 50,000 Sheet 153, Großglockner*. Geologische Bundesanstalt Vienna.

Kaab, A. & C. Kneisel 2006: Permafrost creep within a recently deglaciated glacier forefield: Muragl, Swiss Alps. *Permafrost and Periglacial Processes* 17, 1: 79–85.

Keuschnig, M., I. Hartmeyer, J.-C. Otto & L. Schrott 2011: A new permafrost and mass movement monitoring test site in the Eastern Alps – Concept and first results of the MOREXPERT project. In: Borsdorf, A., J. Stötter & E. Veulliet (eds.): *Managing Alpine Future II – Inspire and drive sustainable mountain regions, Proceedings of the Innsbruck Conference, November 21–23, 2011.* IGF-Forschungsberichte 4. Innsbruck: 163–173.

Kneisel, C. 2003: Permafrost in recently deglaciated glacier forefields measurements and observations in the eastern Swiss Alps and northern Sweden. *Zeitschrift Fur Geomorphologie* 47, 3: 289–305.

Kneisel, C. & A. Kääb 2007: Mountain permafrost dynamics within a recently exposed glacier forefield inferred by a combined geomorphological, geophysical and photogrammetrical approach. *Earth Surface Processes and Landforms* 32, 12: 1797–1810.

Lugon, R., R. Delaloye, E. Serrano, E. Reynard, C. Lambiel & J.J. Gonzalez-Trueba 2004: Permafrost and Little Ice Age glacier relationships, Posets Massif, Central Pyrenees, Spain. *Permafrost and Periglacial Processes* 15, 3: 207–220.

Lunardini, V.J. 1995: Permafrost Formation Time. In: US Army Corps of Engineers – Cold Regions Research and Engineering Laboratory (ed.): *CRREL Report* 95-8.

Ravanel, L. & P. Deline 2011: Climate influence on rockfalls in high-Alpine steep rockwalls: The north side of the Aiguilles de Chamonix (Mont Blanc massif) since the end of the 'Little Ice Age'. *The Holocene* 21, 2: 357–365.

Sattler, K., M. Keiler, A. Zischg & L. Schrott 2011: On the Connection between Debris Flow Activity and Permafrost Degradation: A Case Study from the Schnalstal, South Tyrolean Alps, Italy. P*ermafrost and Periglacial Processes* 22, 3: 254–265.

Schmidt, S., B. Weber & M. Winiger 2009. Analyses of seasonal snow disappearance in an alpine valley from micro- to meso-scale (Loetschental, Switzerland). *Hydrological Processes* 23, 7: 1041–1051.

Schoeneich, P. 2011: GST – Ground surface Temperature, Permanet Guidelines for Monitoring. http://www.permanet-alpinespace.eu/archive/pdf/GST.pdf (accessed: 3.3.2014).

Schrott, L., J.-C. Otto & F. Keller 2012: Modelling alpine permafrost distribution in the Hohe Tauern region, Austria. *Austrian Journal of Earth Science* 105, 2: 169–183.

Suter, S. 2001: *Cold Firn and Ice in the Monte Rosa and Mont Blanc Areas: Spatial Occurrence, Surface Energy Balance and Climatic Evidence*. PhD thesis. Swiss Federal Institute of Technology Zurich ETH Zürich.

Suter, S., M. Laternser, W. Haeberli, R. Frauenfelder & M. Hoelzle 2001: Cold firn and ice of high-altitude glaciers in the Alps: measurements and distribution modelling. *Journal of Glaciology* 47, 156: 85–96.

WGMS 2012: Fluctuations of Glaciers 2005–2010 (Vol. X). In: Zemp, M., H. Frey, I. Gärtner-Roer, S.U. Nussbaumer, M. Hoelzle, F. Paul & W. Haeberli (eds.): *ICSU (WDS)/IUGG (IACS)/UNEP/UNESCO/WMO, World Glacier Monitoring Service, Zürich, Switzerland*. Based on database version doi:10.5904/wgms-fog-2012-11.